Core-shell Yagi-Uda nanoantenna for highly efficient and directive emission

Citation for the original published paper (version of record):
Sergaeva, O., Savelev, R., Baranov, D. et al (2017). Core-shell Yagi-Uda nanoantenna for highly efficient and directive emission. Journal of Physics: Conference Series, 929(1).
http://dx.doi.org/10.1088/1742-6596/929/1/012066

(article starts on next page)

Journal of Physics: Conference Series

PAPER • **OPEN ACCESS**

Core-shell Yagi-Uda nanoantenna for highly efficient and directive emission

To cite this article: Olga N. Sergaeva *et al* 2017 *J. Phys.: Conf. Ser.* **929** 012066

IOP Conf. Series: Journal of Physics: Conf. Series **929** (2017) 012066 doi:10.1088/1742-6596/929/1/012066

Core-shell Yagi-Uda nanoantenna for highly efficient and directive emission

Olga N. Sergaeva[1,2], **Roman S. Savelev**[1], **Denis G. Baranov**[3,4], **Alexander E. Krasnok**[1,5]

[1]ITMO University, St. Petersburg 197101, Russia
[2]Department of Mechanical and Aerospace Engineering, University of Missouri, Columbia, MO, 65211, USA
[3]Department of Physics, Chalmers University of Technology, 412 96 Gothenburg, Sweden
[4]Moscow Institute of Physics and Technology, 9 Institutskiy per., Dolgoprudny 141700, Russia
[5]Department of Electrical and Computer Engineering, The University of Texas at Austin, Austin, Texas 78712, USA

E-mail: r.savelev@metalab.com

Abstract. We study radiation from hybrid Yagi-Uda nanoantennas composed of metal-dielectric core-shell nanoparticles. We show that due to the presence of two types of resonances in each particle at close frequencies the hybrid Yagi-Uda nanoantenna can operate in two different regimes. In the first regime at low frequencies it operates similarly to plasmonic and all-dielectric Yagi-Uda nanoantennas, and it is characterized with highly directive emission in a forward direction. In the second regime at higher frequencies the hybrid nanoantenna can emit with a high directivity in backward direction due to the presence of the hybrid dispersion branch with negative group velocity. Moreover by choosing the appropriate nanoantenna parameters one can achieve the operation regime when due to excitation of dark magnetic dipole modes in nanoantenna high values of directivity and Purcell factor are realized simultaneouslly in extremely narrow frequency range.

1. Introduction

Optical nanoantennas enable enhancement and flexible manipulation of light on the scale much smaller than free space wavelength [1, 2]. Due to this ability, they offer unique opportunities for applications such as optical communications [3], photovoltaics [4], non-classical light emission [5], subwavelength light confinement and enhancement [6], sensing [7], and single-photon sources [8]. A specific type of optical nanoantenna, the Yagi-Uda one, has recently received a widespread attention in the literature [9]. Such nanoantennas consist of several small scatterers and operate similarly to their radio frequency analogues. Yagi-Uda nanoantennas composed of different scatterers, such as core-shell nanoparticles [10], plasmonic nanoparticles [11], high-index dielectric nanoparticles [12] were studied recently. Regardless of the scatterers type, such nanoantennas are characterized by a high directivity in a relatively wide frequency range. Explanation for such behaviour, based on the chain eigenmode analysis was given in Ref. [11] for plasmonic nanoparticles, while it can be also applied to any type of scatterer with a dominant dipole response.

Usually, a Yagi-Uda nanoantenna consists of a reflector and one or several directors. However, as it was pointed out in the Ref. [13], a Yagi-Uda nanoantenna composed of core-

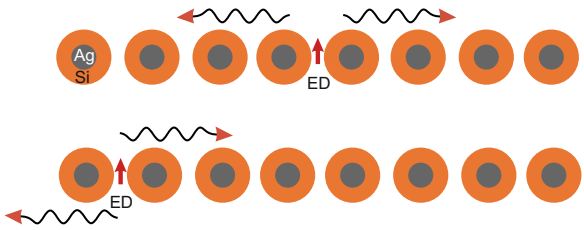

Figure 1. Schematic of the Yagi-Uda nanoantenna – a chain of metal-dielectric core-shell nanoparticles placed with period a. An electric dipole emitter is placed in the center of the chain orthogonally to the chain axis.

shell nanoparticles with both electric dipole (ED) and magnetic dipole (MD) resonant responses at the same frequency does not need a reflector particle, since backward scattering is suppressed automatically, due to Kerker effect [14]. Despite such special feature, core-shell Yagi-Uda nanoantennas still have not been studied in details by now.

Here, we report the results of the theoretical investigation regarding the capabilities of Yagi-Uda nanoantennas composed of Ag-Si core-shell nanoparticles for tailoring the radiation of electric dipole emitters. We show that such hybrid metal-dielectric nanoantenna can operate in two different regimes. In the first regime core-shell nanoantenna operates similarly to the well-known plasmonic and dielectric ones, and it is characterized by very high directivity and low Purcell factor in the wide spectral range at low frequencies. Due to presence of both ED and MD resonances in a single core-shell nanosphere another operation regime is possible. In this regime effective excitation of dark magnetic dipole modes in the chain of core-shell particles by ED source allows one to achieve both high directivity and high Purcell factor in a very narrow frequency range.

2. Electromagnetic properties of core-shell nanoparticles

As an element of the Yagi-Uda nanoantenna, we consider a core-shell nanoparticle with a silver (Ag) core and a silicon (Si) shell. Bi-material core-shell nanoparticles find a broad range of applications in catalysis, nanoelectronics, and biophotonics [15, 16]. They also offer a flexible platform for manipulation of electromagnetic radiation [17, 13]. In contrast to single-material solid particles, the spectral positions of the ED and MD resonances can be tuned almost independently in wide range of frequencies by tuning their geometrical parameters, what makes such particles an advantageous building block for constructing functional nanophotonic devices. Because of the great interest in core-shell particles from the perspective of their unique electromagnetic properties, different methods of their fabrication are being developed [18, 19, 20].

To describe the electromagnetic response of an array of the core-shell nanoparticles under consideration we use the well-known coupled-dipole approximation where each particle is characterized by electric dipole (ED) response (due to core plasmonic particle) and magnetic dipole (MD) response (due to high index dielectric shell). Dipole model for a one-dimensional array of identical particles formulates as follows [21, 22]:

$$\begin{cases} \mathbf{p}_n = \alpha_e(\omega)(\mathbf{E}_n^{(\mathrm{loc})} + \mathbf{E}_n^{(\mathrm{ext})}), \\ \mathbf{m}_n = \alpha_m(\omega)(\mathbf{H}_n^{(\mathrm{loc})} + \mathbf{H}_n^{(\mathrm{ext})}), \end{cases} \tag{1}$$

where $\mathbf{m}_n$ and $\mathbf{p}_n$ are magnetic and electric moments induced in the nth particle ($\propto -i\omega t$), α_m and α_e are magnetic and electric polarizabilities, electric $\mathbf{E}_n^{(\mathrm{ext})}$ and magnetic $\mathbf{H}_n^{(\mathrm{ext})}$ fields at the position of the nth dipole are produced by external source; local electric $\mathbf{E}_n^{(\mathrm{loc})}$ and magnetic

$\mathbf{H}_n^{(\mathrm{loc})}$ fields are produced by all other dipoles in the chain:

$$\begin{cases} \mathbf{E}_n^{(\mathrm{loc})} = \sum\limits_{j\neq n} \left(\widehat{C}_{nj}\mathbf{p}_j - \widehat{G}_{nj}\mathbf{m}_j \right), \\ \mathbf{H}_n^{(\mathrm{loc})} = \sum\limits_{j\neq n} \left(\widehat{C}_{nj}\mathbf{m}_j + \widehat{G}_{nj}\mathbf{p}_j \right), \end{cases} \tag{2}$$

where $\widehat{C}_{nj} = A_{nj}\widehat{I} + B_{nj}(\widehat{\mathbf{r}}_{nj} \otimes \widehat{\mathbf{r}}_{nj})$, $\widehat{G}_{nj} = -D_{nj}\widehat{\mathbf{r}}_{nj} \times \widehat{I}$, $\otimes$ is a dyadic product, $\widehat{I}$ is the unit 3×3 tensor, $\widehat{\mathbf{r}}_{nj}$ is the unit vector in the direction from nth to jth dipole; $A_{nj} = e^{ik_hR_{nj}}\left(\frac{k_h^2}{R_{nj}} - \frac{1}{R_{nj}^3} + \frac{ik_h}{R_{nj}^2}\right)$, $B_{nj} = e^{ik_hR_{nj}}\left(-\frac{k_h^2}{R_{nj}} + \frac{3}{R_{nj}^3} - \frac{3ik_h}{R_{nj}^2}\right)$, $D_{nj} = e^{ik_hR_{nj}}\left(\frac{k_h^2}{R_{nj}} + \frac{ik_h}{R_{nj}^2}\right)$, where R_{nj} is the distance between the nth and jth dipoles, ε_h is the permittivity of the host medium (in our calculations we take $\varepsilon_h = 1$), and $k_h = \sqrt{\varepsilon_h}\omega/c$ is the wavenumber in the host medium, $\omega = 2\pi\nu$, ν is the frequency, and c is the speed of light. Electric and magnetic polarizabilities are defined as $\alpha_e = i\frac{3\varepsilon_h a_1^{sc}}{2k_h^3}$, $\alpha_m = i\frac{3b_1^{sc}}{2k_h^3}$, where scattering coefficients a_1, b_1 can be expressed via the parameters of the layered particle [23].

The Ag-Si particles exhibit resonant dipole responses in near infrared frequency range [17]. Using the radius of the silver core $R_c = 68$ nm and the radius of the silicon shell $R = 225$ nm,

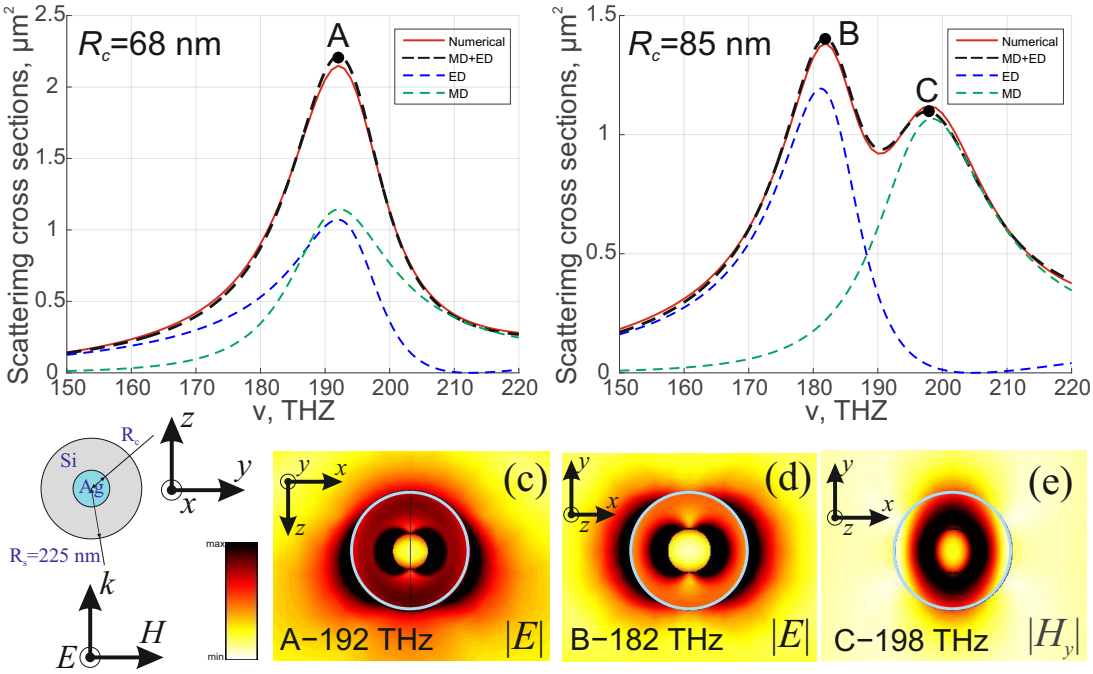

Figure 2. (a,b) Scattering cross-sections (solid red and dashed black curves) for Ag-Si core-shell particles with $R_s = 225$ nm and (a) $R_c = 68$ nm and (b) $R_c = 85$ nm. Dashed black curves are calculated within the framework of the dipole model, and red curves are obtained via full-wave numerical simulation. Partial ED and MD contributions are shown with dashed blue and green curves, respectively. (c-e) Field amplitude distributions at different frequencies: (c) point "A" in (a) (192 THz), (d) point "B" in (b) (182 THz), (e) point "C" in (b) (198 THz), indicating ED+MD, ED and MD resonances, respectively.

the overlap of the ED and MD resonances of the Ag-Si core-shell nanoparticle can be achieved. We assume constant permittivity of silicon $\varepsilon_s = 11.56$, and for the dispersion of silver core we employed Drude model $\varepsilon_c(\nu) = 1 - \nu_p^2/(\nu^2 + i\gamma\nu)$, with plasma frequency $\nu_p = 2180$ THz and collision frequency $\gamma = 4.93$ THz. At the frequency range of interest it very well matches the experimental data given in Ref. [24]. The extinction cross sections of an x-polarized plane wave by core-shell nanoparticle with these parameters along with its partial ED and MD contributions is shown in Figs. 2(a,b) for $R_c = 68$ nm and $R_c = 85$ nm, respectively. The electric field at the resonance frequency in Fig. 2(a) (point "A") combines characteristic field distributions of both ED and MD resonances: namely, strongly enhanced electric field near the core due to the ED plasmonic resonance and slightly enhanced circular distributed electric field due to MD resonance in high-index dielectric shell [see Fig. 2(c)]. Increase of the core radius from 68 nm to 85 nm shifts the ED resonance frequency to ≈182 THz [point "B" in Fig. 2(b)] and MD resonance frequency to ≈198 THz [point "C" in Fig. 2(b)] with corresponding field distributions plotted in Figs. 2(d,e), respectively. This demonstrates the possibility of the efficient tuning the frequencies of the two main resonances of hybrid core-shell particles by simple change of their geometrical parameters.

3. Yagi-Uda core-shell nanoantennas

It is known that far fields produced by magnetic and electric point dipoles cancel each other in backward of forward direction if they have the same amplitude and are oscillating in or out of phase, respectively [14]. Since the backscattering is suppressed automatically in the case of particles with overlapping MD and ED resonances, the Yagi-Uda nanoantenna composed of such elements does not require a reflector [13]. According to this, we place a point electric dipole source (emulating a quantum emitter) oriented orthogonally to the axis of the chain of 8 core-shell nanospheres with $R_c = 68$ nm and $R_s = 225$ nm placed with period $a = 550$ nm. Directivity of a nanoantenna can be calculated within the framework of this model [25]: $D_{\mathbf{max}} = \dfrac{4\pi \cdot \max[p(\theta,\varphi)]}{P_{rad}}$, where $\max[p(\theta,\varphi)]$ is the power transmitted in the direction of the main lobe, and $P_{rad} = \int p(\theta,\varphi) d\Omega$ is the total power radiated by a system into the far zone. Frequency dependent directivity for the considered nanoantenna is shown in Fig. 3(a). In order to understand the origin of highly directive emission at low frequencies, following the Koenderink analysis [11] we calculate dispersion properties of an infinite core-shell nanospheres chain. Eigenmodes can be calculated from the analytical closed-form dispersion equations that can be obtained by replacing infinite sums in (2) with analytical functions [26, 27]. In Fig. 3(b) one can observe, that the low frequency chain eigenmode is close to the light line at frequencies $\lesssim$ 170 THz (far from the particle resonances), which corresponds to the high directivity frequency range in Fig. 3(a). Besides the low frequency dispersion branch, due to the presence of two types of resonances there is also a second dispersion branch, which crosses the light line at ≈ 195 THz. For the considered parameters, EDs and MDs amplitudes of the chain eigenmodes are of the same order of magnitude for both branches and consequently there is a strong MD-ED interaction between the neigbour particles. Due to this interaction, the second branch is characterized by a negative group velocity and at the frequency near 195 THz, which corresponds to the observed peak in directivity, the nanoantenna radiates in backward direction [see inset in Fig. 3(a)].

The conventional operation regime of Yagi-Uda nanoantennas at low frequencies is naturally nonresonant. This can be understood from the eigenmode analysis of the considered structure. Eigenfrequencies of the chain of 8 particles with real part below 170 THz [corresponding to the first dispersion branch in Fig. 3(b)], have very large imaginary parts, and thus low frequency operation regime of Yagi-Uda nanoantenna is broadband and nonresonant. Consequently, another important property of nanoantennas, namely Purcell factor (PF), is quite low in this regime [12]. We confirmed it by calculating the PF with the well-known formula [25]

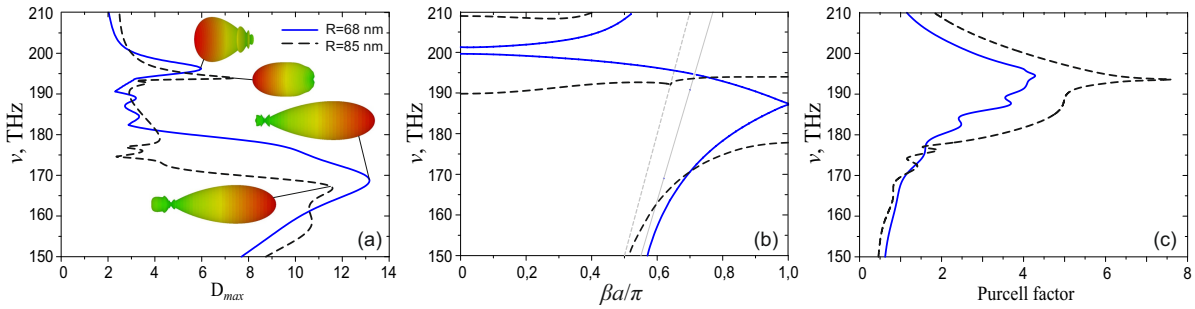

Figure 3. (a) Directivity and (c) Purcell factor for the chain of 8 core-shell nanoparticles with dipole source located on the axis of the chain at the half period from the center of the leftmost particle. (b) Dispersion diagram for the transversely polarized modes of an infinite chain of core-shell nanoparticles; $\beta a/\pi$ is the normalized Bloch wave number and ν is the frequency. Solid blue (dashed black) curves correspond to the following parameters: radius of Ag core $R_c = 68$ nm ($R_c = 85$ nm), radius of silicon shell $R_s = 225$ nm and the period of the chain $a = 550$ nm ($a = 500$ nm).

$F = 1 + \frac{3}{2k^3d^2}\mathrm{Im}\,[\mathbf{d}^* \cdot \mathbf{E}_s]$, where k is the wave number, $\mathbf{d}$ is the dipole moment of the emitter, and $\mathbf{E}_s$ is the scattered electric field at the position of the source. Results of calculations are shown in Fig. 3(c): values of the PF at low frequencies do not exceed 1. The eigenfrequencies of the finite chain that correspond to the second dispersion branch, which is close to the resonances of the single particle, have small imaginary parts and therefore we call this operation regime. In the resonant regime the PF is much higher than in the nonresonant one, but the values of PF are still quite low $\lesssim$10.

In order to increase the PF and consequently the antenna efficiency we employ the method of magnetic dark chain eigenmodes excitation [28]. This method relies on the symmetry matching of the ED source oriented perpendicular to the chain axis and the staggered eigenmode of the chain of MDs, i.e. with MD moments in neighbouring nanoparticles oscillating out-of-phase. However, if the source is placed outside the chain, the modes excitation is not very effective, which is the case, demonstrated in Fig. 3 for the particles with two different radii of the core: in both cases the maximum of the directivity and the PF are quiet low in the resonant operation regime.

According to this, we calculated the PF and directivity for another two different positions of the source: in the center of the chain, and between the first and the second particles. For the case of $R_c = 68$ nm the directivity and the PF in the narrow frequency range corresponding to the resonant operating regime are shown in Figs. 4(a,b). Despite that for these positions of the source the chain eigenmodes are excited more effectively, we observe only a ≈4-fold increase in the PF, while the directivity decreases overall.

There are two reasons why increase of the Purcell factor in this case is not very large. First reason is the unique dispersion properties of the chain of hybrid MD+ED dipoles chain near the edge of the Brillouin zone. In the chain of particles with only one dominant dipole response (ED or MD) the group velocity tends to zero and, consequently, the density of photonics states diverges at the *Van Hove singularity* near the edge of the Brillouin zone (in the lossless case) [28]. However, when the particles exhibit both MD and ED resonances at the same frequency, there is no gap between the dispersion branches [see Fig. 3(b)]. Since Purcell factor is proportional to the density of photonics states, very high values of the PF cannot be achieved in the chain of core-shell nanoparticles with the fully spectrally overlapping MD and ED resonances.

Second, while there is a symmetry matching between the magnetic field of electric dipole

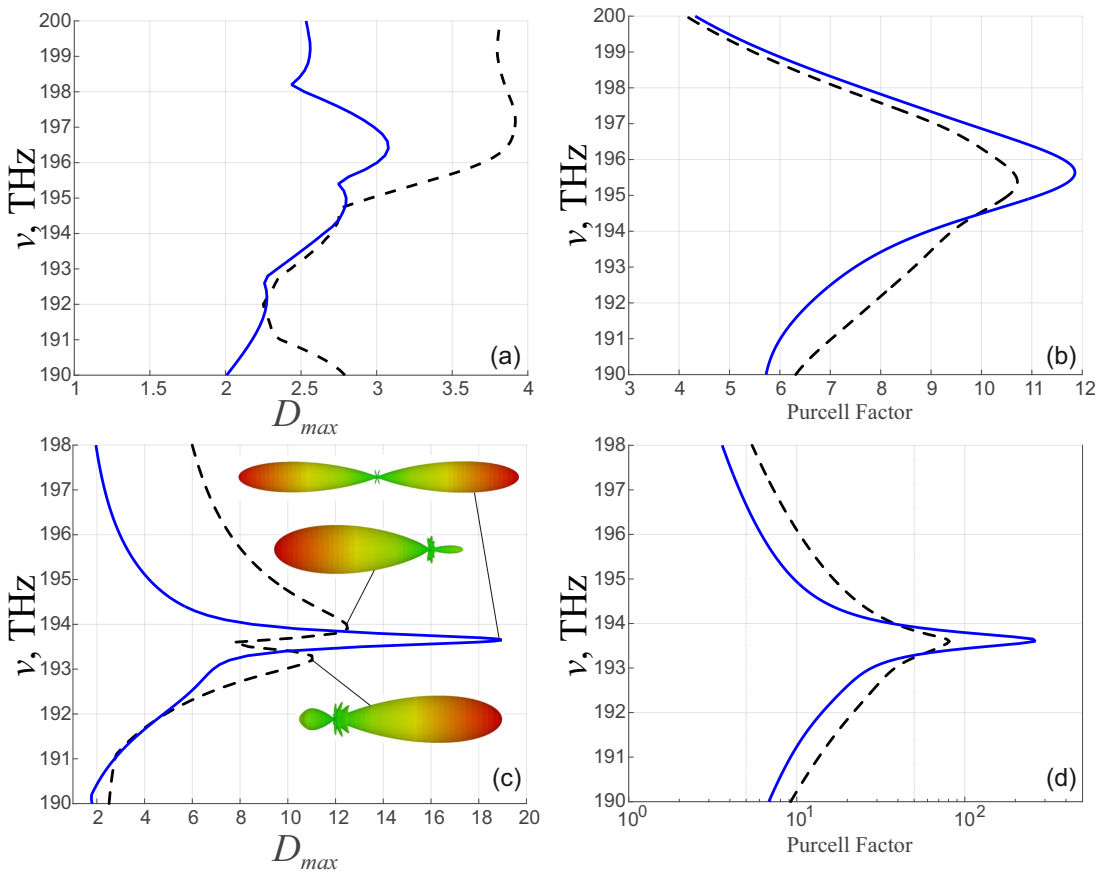

Figure 4. (a,c) Directivity and (b,d) Purcell factor for the chain of 8 core-shell nanoparticles with dipole source located in the middle of the chain (solid blue curves) and between the two leftmost particles (dashed black curves). (a,b) correspond to the $R_c = 68$ nm radius of Ag core, period of the chain is $a = 550$ nm and; (c,d) — to the $R_c = 85$ nm, period of the chain is $a = 500$ nm.

source placed between the particles and MD moments distribution of the staggered chain eigenmode, corresponding electric field and ED moments symmetrically mismatch. Since MD and ED moments in this case are of the same order of magnitude, this also decreases the efficiency of excitation of these modes with electric dipole source.

A different situation is observed for the core-shell particles with $R = 85$ nm. In contrast to the case of $R = 68$ nm, now the second branch is characterized by zero group velocity at the edge of the Brillouin zone, and an infinite local density of optical states [see Fig. 3(b)]. Moreover, the amplitudes of MD moments are substantially larger than amplitudes of ED moments for the second dispersion branch. Therefore, these eigenmodes can be effectively excited with ED source, which allows to achieve both high directivity and high rate of ED source emission in the same frequency range. Note, that since we are interested in the emission of ED source, MD resonance frequency should be higher than ED one. This is so, because the first dispersion branch is characterized with qualitatively the same behaviour for different relative position of resonances and the frequency ranges of high directivity and high Purcell factor do not overlap. While the second dispersion branch can be engineered in different ways.

For the case of $R = 85$ nm, shown in Figs. 4(c,d), we observe that dipole, placed in the center of the chain, emits in both backward and forward directions along the chain with high directivity

≈19 [see insets in Fig. 4(c)], while the PF for this configuration reaches high values up to 270 due to the high density of photonic states at the Van Hove singularity. Emission in a certain direction can be achieved by placing the source between first and second particles [dashed curve in Fig. 4(c)]. In this case the PF is almost one order lower, but source emits predominantly in one direction at certain frequencies [see insets in Fig. 4(c)].

4. Conclusion

To conclude, we have studied emission properties of a dipole source coupled to the Yagi-Uda nanoantenna composed of core-shell nanoparticles. We have demonstrated that the radiation pattern and the emission rate of the nanoantenna fed with electric dipole source strongly depend on the relative position of ED and MD resonance frequencies of a single particle. For most parameters, the hybrid core-shell nanoantenna operates as a conventional Yagi-Uda antenna without reflector, exhibiting highly directive emission in wide frequency range. For certain parameters, almost flat dispersion of the infinite chain of core-shell nanoparticles with inherent high density of photonic states can be realized. In this regime, high values of the Purcell factor and highly directive emission pattern of the nanoantenna can be achieved simultaneously. Finally, while our design of the hybrid nanoantenna is very simple from theoretical point of view, it implies the fabrication of spherical core-shell nanoparticles with high precision, which might be extremely difficult considering current state of technologies. We expect that predicted effects can also be achieved in similar hybrid structures with comparable electromagnetic properties that require simpler fabrication processes [29, 30].

5. ACKNOWLEDGMENTS

This work was supported by RFBR, according to the research projects No. 16-37-60092 mol_a_dk, No. 16-37-60076 mol_a_dk and No. 16-32-00444 mol_a and by Grant from the President of the Russian Federation (MK-381.2017.2).

References

[1] Novotny L and van Hulst N 2011 *Nature Photon.* **5** 83–90
[2] Agio M and Alù A 2013 *Optical antennas* (Cambridge University Press, Cambridge)
[3] Alù A and Engheta N 2010 *Phys. Rev. Lett.* **104**(21) 213902
[4] Atwater H and Polman A 2010 *Nature Materials* **9** 205–213
[5] Maksymov I S, Besbes M, Hugonin J P, Yang J, Beveratos A, Sagnes I, Robert-Philip I and Lalanne P 2010 *Phys. Rev. Lett.* **105**(18) 180502
[6] Stockman M 2004 *Phys. Rev. Lett.* **93** 137404
[7] Liu N, Tang M, Hentschel M, Giessen H and Alivisatos A 2011 *Nature Materials* **10** 631–636
[8] Buckley S, Rivoire K and Vuckovic J 2012 *Reports on Progress in Physics* **75** 126503
[9] Krasnok A, Maksymov I, Denisyuk A, Belov P, Miroshnichenko A, Simovski C and Kivshar Y 2013 *Physics-Uspekhi* **56** 539–564
[10] Li J, Salandrino A and Engheta N 2007 *Phys. Rev. B* **76**(24) 245403
[11] Koenderink A F 2009 *Nano Letters* **9** 4228–4233
[12] Krasnok A E, Miroshnichenko A E, Belov P A and Kivshar Y S 2012 *Opt. Express* **20** 20599–20604
[13] Liu W, Miroshnichenko A, Neshev D and Kivshar Y 2012 *ACS Nano* **6** 5489–5497
[14] Kerker M, Wang D S and Giles C L *J. Opt. Soc. Am.*
[15] Zhong C J and Maye M M 2001 *Advanced Materials* **13** 1507–1511
[16] Ghosh Chaudhuri R and Paria S 2012 *Chemical Reviews* **112** 2373–2433
[17] Paniagua-Domínguez R, López-Tejeira F, Marqués R and Sánchez-Gil J A 2011 *New Journal of Physics* **13** 123017
[18] Ghoshal T, Biswas S and Kar S 2008 *The Journal of Physical Chemistry C* **112** 20138–20142
[19] Zograf G P, Zuev D A, Milichko V A, Mukhin I S, Baranov M A, Ubyivovk E V, Makarov S V and Belov P A *Journal of Physics: Conference Series* **741** 012119
[20] Zograf G P, Rybin M V, Zuev D A, Makarov S V, Belov P A, Lopanitsyna N Y, Kuksin A Y and Starikov S V 2016 *Days on Diffraction (DD)* 460–463
[21] Mulholland G W, Bohren C F and Fuller K A 1994 *Langmuir* **10** 2533–2546

[22] Merchiers O, Moreno F, González F and Saiz J M 2007 *Phys. Rev. A* **76**(4) 043834
[23] Aden A and Kerker M 1951 *Journal of Applied Physics* **22** 1242–1246
[24] Johnson P B and Christy R W 1972 *Phys. Rev. B* **6**(12) 4370–4379
[25] Novotny L and Hecht B 2006 *Principles of Nano-Optics* (Cambridge University Press)
[26] Savelev R, Slobozhanyuk A, Miroshnichenko A, Kivshar Y and Belov P 2014 *Phys. Rev. B* **89** 035435
[27] Shore R A and Yaghjian A D 2012 *Radio Science* **47**
[28] Krasnok A E, Glybovski S B, Petrov M I, Makarov S V, Savelev R S, Belov P A, Simovski C R and Kivshar Y S 2016 *Appl. Phys. Lett.* **108** 211105
[29] Rusak E, Staude I, Decker M, Sautter J, Miroshnichenko A E, Powell D A, Neshev D N and Kivshar Y S 2014 *Appl. Phys. Lett.* **105** 221109
[30] Zuev D A, Makarov S V, Mukhin I S, Milichko V A, Starikov S V, Morozov I A, Shishkin I I, Krasnok A E and Belov P A 2016 *Advanced Materials* **28** 3087–3093